Modeling and Simulation of Shanghai MAGLEV Train Transrapid with Random Track Irregularities

Prof. Shu Guangwei M.Sc.

Prof. Dr.-Ing. Reinhold Meisinger

Prof. Shen Gang Ph.D.

Shanghai Institute of Technology, Shanghai, P.R. China

Nuremberg University of Applied Sciences, Nuremberg, Germany

Tongji University, Shanghai, P.R. China

Abstract

The MAGLEV Transrapid is a kind of new type high speed train in the world which is levitated and guided over the track using electro magnetic forces. Because the electro magnets are unstable, they have to be controlled. Since 2002 the worldwide first commercial use of such a high speed train based on German technology is running successfully in Shanghai Pudong Airport, P.R.China.
In this paper modeling of the high speed MAGLEV train Transrapid is discussed, which considered the whole mechanical system of one vehicle with optimized suspension parameters and all controlled electro magnet pairs in vertical and lateral directions. The dynamical simulation code is generated with MATLAB/SIMILINK. For the design of the control system, the optimal Linear Quadratic Control for minimum control energy is used for each single electro magnet. The simulation results are presented with the given vertical and lateral random track irregularities.

The research work was carried out together with Prof. Shen Gang, Ph.D. during the time Prof. Dr. Meisinger was visiting professor in Shanghai 2006 and Prof. Shu Guangwei, M.Sc. was visiting professor in Nuremberg 2007.

ISSN 1616-0762 Sonderdruck Schriftenreihe der Georg-Simon-Ohm-Fachhochschule Nürnberg Nr. 39, Juli 2007

1. Introduction

In order to improve the ride quality of the Shanghai MAGLEV train, an investigation has been carried out on the possible optimization of passive suspensions and alternative control strategies with the aid of computer simulations. Hence a designated simulation model is created to achieve reasonable balance between accuracy, efficiency and cost effectiveness.
There are many computer models created for different purposes [1,3,6,8,10], generally which can be classified into the following categories: models for design magnetic levitation control [1,2,3,5], models for suspension optimization [4], models for track-train interaction [3,5,6,12]. Depending on various requirements the scales of the models vary in fidelity from a single magnetic block [1,3,7] to the whole train system [6,8].
Regarding the tools of computer software, there are commercial software packages such as SIMPACK, ADAMS,etc. [9,10,11], and also self generated codes [3,5,6,7,8,12].
The principle idea behind modeling in this paper is to develop a whole vehicle model with detailed suspension elements and practical controller with a reasonable description of the track irregularities, without coupling to the guideway.

2. Mechanical System Model

The train consists of five sections, each section consists of a car body and running gears which connects the levitation and guidance magnets. The running gear is also called Magnetic Wheels. Two adjacent Magnetic Wheels are connected to form a so-called levitation bogie. There are four such levitation bogies under a car body. The levitation bogies are designed to enable transmission of vertical forces to support the car body and to transmit lateral forces to guide the train, transmission of longitudinal forces provides for braking and traction forces. Consequently it is a very important component in the vehicle for both safety and comfort.

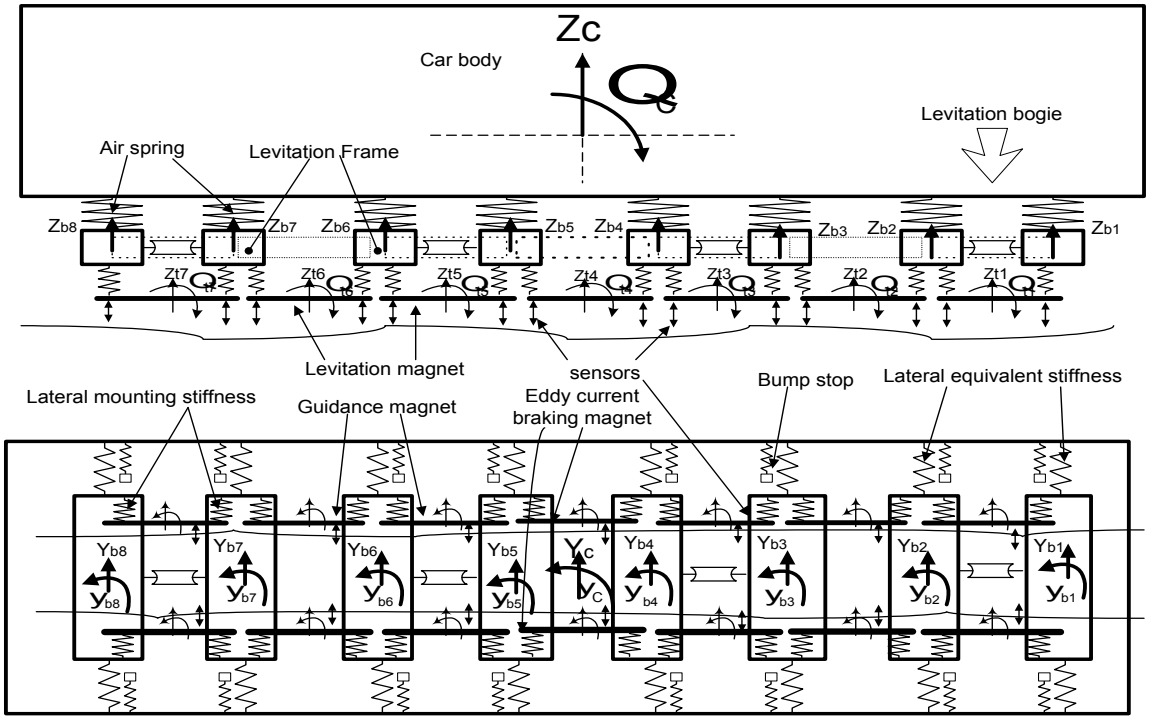

Fig. 1: Side view of the model

There are many suspension elements within the levitation bogie, for example, two air springs, anti-roll bars and rubber elements, primary metal-rubber elements which connect the levitation magnets, lateral bump stop metal-rubber elements, metal-rubber elements which connect the braking magnets, etc.. The car body is connected vertically by 16 swing-rods that provide lateral flexibility. There are two rubber stacks at one end of the

swing-rods to give flexibility in the axial direction. The longitudinal forces are transmitted by 4 traction rods to the four frames separately. These suspension elements isolate most disturbances from the guiding track, both vertically and laterally.
A vehicle model is created considering 5 degrees of freedom for the car body and 4 degrees of freedom for each magnetic levitation frame and 2 degrees of freedom for each magnet pair. There are eight levitation frames, 14 levitation magnets, 12 guidance magnets and 2 eddy current brake modules for both sides. Totally there are 93 degrees of freedom considered in the mechanical model as show in Figure 1 and 2.

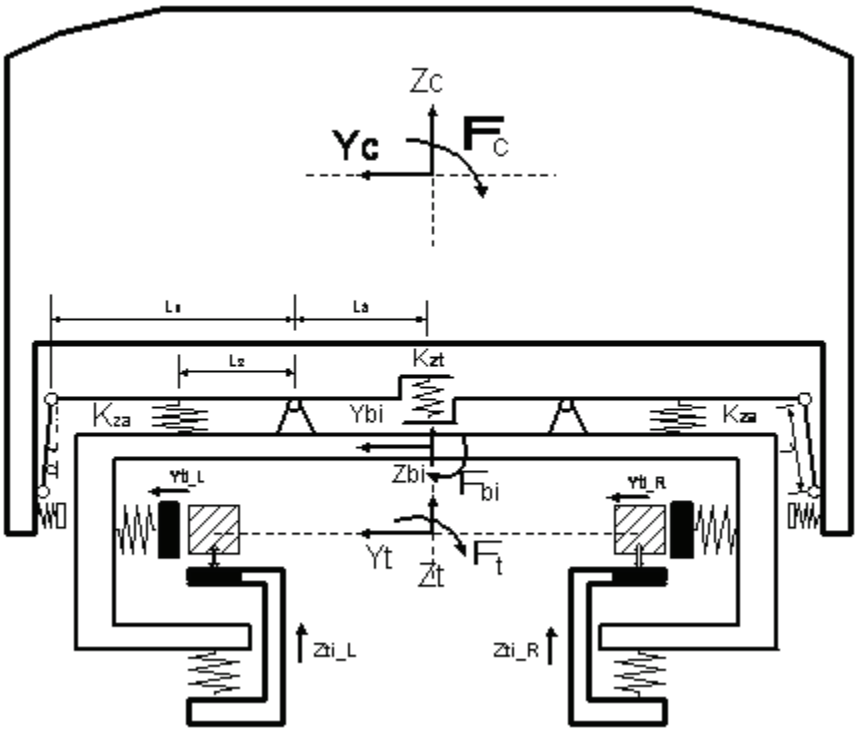

Fig. 2: Cross section of the model

With the assumption of a rigid car body, five degrees for the car body are considered including vertical, lateral, yaw, pitch and rotation movements. There are four levitation bogies beneath the car body, each consists of two relatively rigid frames, called levitation frame. Two levitation frames are connected by a longitudinal structure with relative flexibility and light mass. So the levitation bogie can be treated as two rigid parts (levitation frame) connecting via shear stiffness in the vertical and lateral directions together with a rotational angular stiffness. Each levitation frame is considered with four degrees for vertical, lateral, pitch and rotation movements respectively. Each levitation magnet is suspended from two adjacent levitation frames with relative flexibility vertically and longitudinally. Hence each levitation magnets is considered as having two degrees for vertical and pitch movements respectively. The guidance magnets are also similar to levitation magnets, which are connected to the side of adjacent levitation frames with relative lateral flexibility. The guidance magnets are considered as two degree also, i.e. degrees for lateral and yaw movements respectively.
Secondary suspensions between car body and levitation frames are provided through a combination of air springs, rubbers stacks, swing-rods and rotation arms etc. as shown in Figure 2. The rotation arms and swing-rods are relatively light in weight. Hence it is not necessary to consider their inertial effects. Whole structures can be simplified with three stiffness, i.e. lateral stiffness Kys, roll stiffness Krs and vertical stiffness Kzs. These three parameters are defined as the function of stiffness of air spring, anti-roll stiffness and several geometric dimensions as follows:

$$K_{ys} = \frac{W}{L}; \quad K_{zs} = \frac{L_2^{\,2}}{L_1^{\,2}} K_{za}; \quad K_{rs} = 2(L_1 + L_3)^2 \cdot \left(\frac{L_2^{\,2}}{L_1^{\,2}} K_{za} + 2\frac{L_3^{\,2}}{L_1^{\,2}} K_{zt}\right)$$

Where W is the suspended weight of on each frame. Other parameters are shown in Figure 2.
Primary suspensions are simple in this case. There is only vertical stiffness to the levitation magnets and lateral stiffness to the guidance magnets.
For the practical application, two magnets consist a pair of vertical magnet levitation block with two gap and acceleration sensors for each magnet. The linear quadratic control can be used for minimum control energy with linearized coefficients at the working point [12,13]. The controller can be treated for individual or modal control.

3. Control System Modeling

With the assumption of a single levitated mass as shown in Figure 3, the controller are designed for both levitation and guidance. There m is the levitated mass (including levitation frame and magnet), f is the dynamic magnet force, z_T is the track disturbance and z_t is the magnet deviation. S_0 is the nominal magnet gap, s is the small deviation from the nominal gap, $L_0 = L_e + L_s$ is the whole inductance, with the effective inductance L_e and the constant stray inductance L_s. R is the resistance, I_0 is the nominal current and u is the small deviation from the nominal magnet voltage $R\,I_0$.

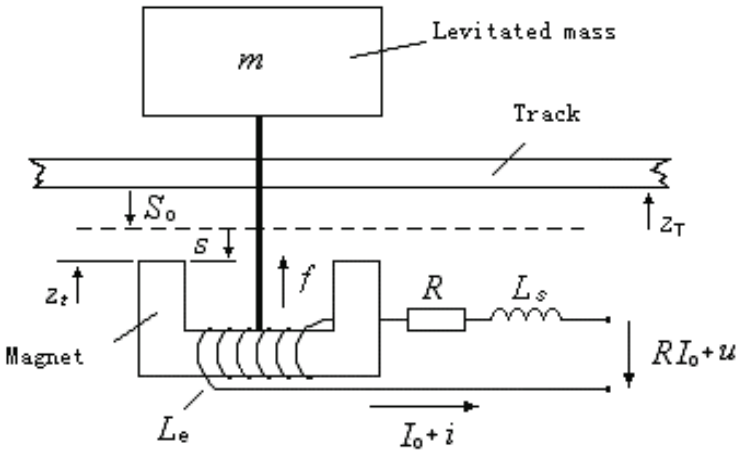

Fig. 3: Model of a single mass vehicle for vertical motion

The linear equation of the single mass magnetic levitation system can be derived with LAGRANGE–Function as shown in [12,13,14,15]:

$$\ddot{s} = -\frac{(1-\eta)}{m} L_0 \frac{I_0}{S_0} i + \frac{(1-\eta)}{m} L_0 \left(\frac{I_0}{S_0}\right)^2 s = -\frac{P_i}{m} i + \frac{P_s}{m} s \tag{1}$$

$$\dot{i} = -\frac{R}{L_0} i + (1-\eta)\frac{I_0}{S_0}\dot{s} + \frac{1}{L_0} u \tag{2}$$

where $\eta = L_s / L_0$, $P_i = \dfrac{(1-\eta)L_0 I_0}{S_0}$, $P_s = \dfrac{(1-\eta)L_0 I_0^2}{S_0^2}$

Considering the dynamic magnet force $f = P_i i - P_s s$, then is

$$\dot{f} = P_i \dot{i} - P_s \dot{s} \tag{3}$$

Substituting eq.(2) into eq.(3) and taking note of $i = \dfrac{P_s}{P_i} s + \dfrac{1}{P_i} f$, there is

$$\dot{f} = -\frac{P_s}{T}s - P_s\eta\dot{s} - \frac{1}{T}f + \frac{(1-\eta)P_s}{P_i}u \tag{4}$$

where $T = L_0/R$ is the time constant. In order to accord with the vehicle coordinate system in Figure 1 and Figure 2 the transformation is made as below:

$$z_t = -s + z_T \;;\; \dot{z}_t = -\dot{s} + \dot{z}_T$$

Selecting magnet deviation z_t, vertical velocity $\dot{z}_t$ and dynamic magnet force f as the state variables, that is $\boldsymbol{x}(t) = \begin{bmatrix} z_t & \dot{z}_t & f \end{bmatrix}^{\mathrm{T}}$, the following state equation is obtained

$$\begin{bmatrix} \dot{z}_t \\ \ddot{z}_t \\ \dot{f} \end{bmatrix} = \begin{bmatrix} 0 & 1 & 0 \\ 0 & 0 & 1/m \\ P_s/T & P_s\eta & -1/T \end{bmatrix} \begin{bmatrix} z_t \\ \dot{z}_t \\ f \end{bmatrix} + \begin{bmatrix} 0 \\ 0 \\ (1-\eta)P_s/P_i \end{bmatrix} u + \begin{bmatrix} 0 & 0 \\ 0 & 0 \\ -P_s/T & -P_s\eta \end{bmatrix} \begin{bmatrix} z_T \\ \dot{z}_T \end{bmatrix} \tag{5}$$

i.e. $\dot{\boldsymbol{x}}(\boldsymbol{t}) = \boldsymbol{A}\boldsymbol{x}(\boldsymbol{t}) + \boldsymbol{B}u(\boldsymbol{t}) + \boldsymbol{E}v(\boldsymbol{t})$

With magnet gap deviation $z_t - z_T$, vertical velocity $\dot{z}_t$ and vertical acceleration $\ddot{z}_t$ as the measurements the following output equation is obtained (in practice $\dot{z}_t$ is computed by an observer [5,12]):

$$\begin{bmatrix} z_t - z_T \\ \dot{z}_t \\ \ddot{z}_t \end{bmatrix} = \begin{bmatrix} 1 & 0 & 0 \\ 0 & 1 & 0 \\ 0 & 0 & 1/m \end{bmatrix} \begin{bmatrix} z_t \\ \dot{z}_t \\ f \end{bmatrix} + \begin{bmatrix} -1 & 0 \\ 0 & 0 \\ 0 & 0 \end{bmatrix} \begin{bmatrix} z_T \\ \dot{z}_T \end{bmatrix} \tag{6}$$

i.e. $\boldsymbol{y}(\boldsymbol{t}) = \boldsymbol{C}\boldsymbol{x}(\boldsymbol{t}) + \boldsymbol{D}v(\boldsymbol{t})$

To optimize the system the quadratic loss criterion

$$J = \frac{1}{2}\int_0^\infty \left[\boldsymbol{x}^{\mathrm{T}}(t)\boldsymbol{C}^{\mathrm{T}}\boldsymbol{Q}\boldsymbol{C}\boldsymbol{x}(t) + \boldsymbol{u}^{\mathrm{T}}(t)\boldsymbol{R}\boldsymbol{u}(t) \right] \mathrm{d}t = \min \tag{7}$$

is used. There $\boldsymbol{Q}$ and $\boldsymbol{R}$ are the weighting matrices with $\boldsymbol{Q} = \mathrm{diag}\begin{bmatrix} q_{11} & q_{22} & q_{33} \end{bmatrix}$.
Then the controller feedback matrix $\boldsymbol{K}$ is obtained as

$$\boldsymbol{K} = \boldsymbol{R}^{-1}\boldsymbol{B}^{\mathrm{T}}\boldsymbol{P} \tag{8}$$

where $\boldsymbol{P}$ can be solved from the matrix RICCATI-equation

$$\boldsymbol{P}\boldsymbol{A} + \boldsymbol{A}^{\mathrm{T}}\boldsymbol{P} - \boldsymbol{P}\boldsymbol{B}\boldsymbol{R}^{-1}\boldsymbol{B}^{\mathrm{T}}\boldsymbol{P} + \boldsymbol{C}^{\mathrm{T}}\boldsymbol{Q}\boldsymbol{C} = 0 \tag{9}$$

Then the optimal feedback control law is

$$\boldsymbol{u}(t) = -\boldsymbol{K}\,\boldsymbol{y}(t) \tag{10}$$

The weightings in eq.(7) used for the control system design for minimum control energy are

$$\boldsymbol{Q} = \mathrm{diag}\begin{bmatrix} 0 & 0 & 0 \end{bmatrix},\ \boldsymbol{R} = 1.$$

The above single mass control model can be applied to each magnet of the simulated MAGLEV vehicle with the optimized parameters for individual and modal control strategies alternatively as shown in Figure 4.
The equation and the design method of guidance control system are similar.

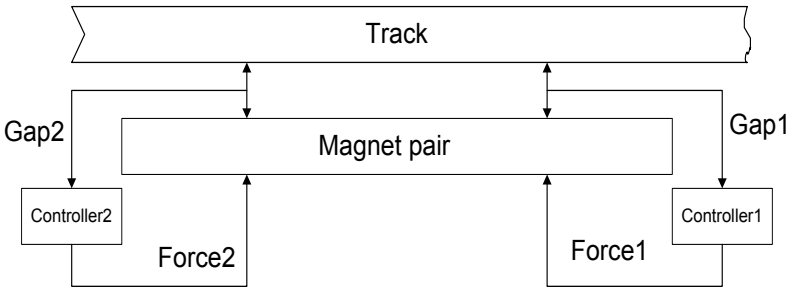

(a) Individual control of the magnet pair

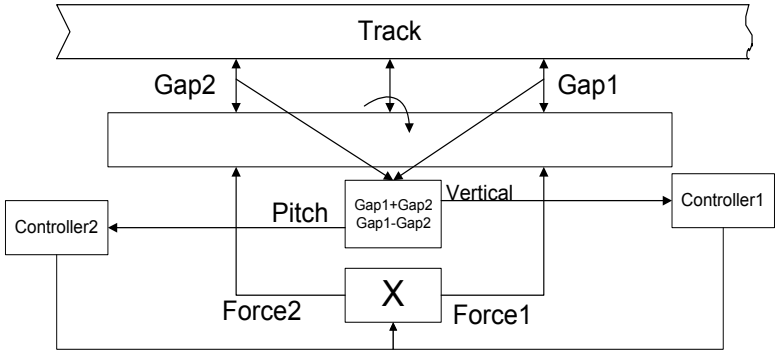

(b) Modal control of the magnet pair

Fig. 4: Alternative control strategies

4. Simulation Code and Main Results

The SIMULINK diagram is shown in the Figure 5. It consists of several subsystem blocks. The most top block is of the car body. Below that there are 8 blocks for secondary suspensions. Then followings are 4 levitation bogie frame blocks, 6 guidance blocks and one brake magnet block, 7 levitation magnet blocks and relevant controller blocks. The inputs to the system are given by track lateral irregularity block and track vertical irregularity block on the left side in the diagram.
As an example, for the case (a) in Figure 4, the controller block diagram for the right side levitation magnet is shown in the Figure 6. Where 'Zt' represents the vertical movement of magnet, and 'Pt' represents the pitch rotation movement of the magnet, 'dt' represents the half space between left and right magnets, 'lt' represents the distance between front point and the rear point of the measurements, 'G' represents $(1-\eta)P_s / P_i$, 'ata' represents η, the elements of the ***K*** in eq.(10) are K1, K2 and K3. The inputs to the block are track irregularities and states of magnet of right side. The output from the block are the magnetic forces acting on the front and rear points of the magnet.

4.1 Track irregularities

Assuming a highly rigid and heavy mass track, the interaction between vehicle and the track can be simplified by just considering first order bending with even load distribution. The track irregularity consists of random surface irregularities and periodic deformations.
It is important to measure the field track irregularities for the MAGLEV system to clarify the differences between the MAGLEV track and railway tracks. It has been indicated that there are differences in different frequency

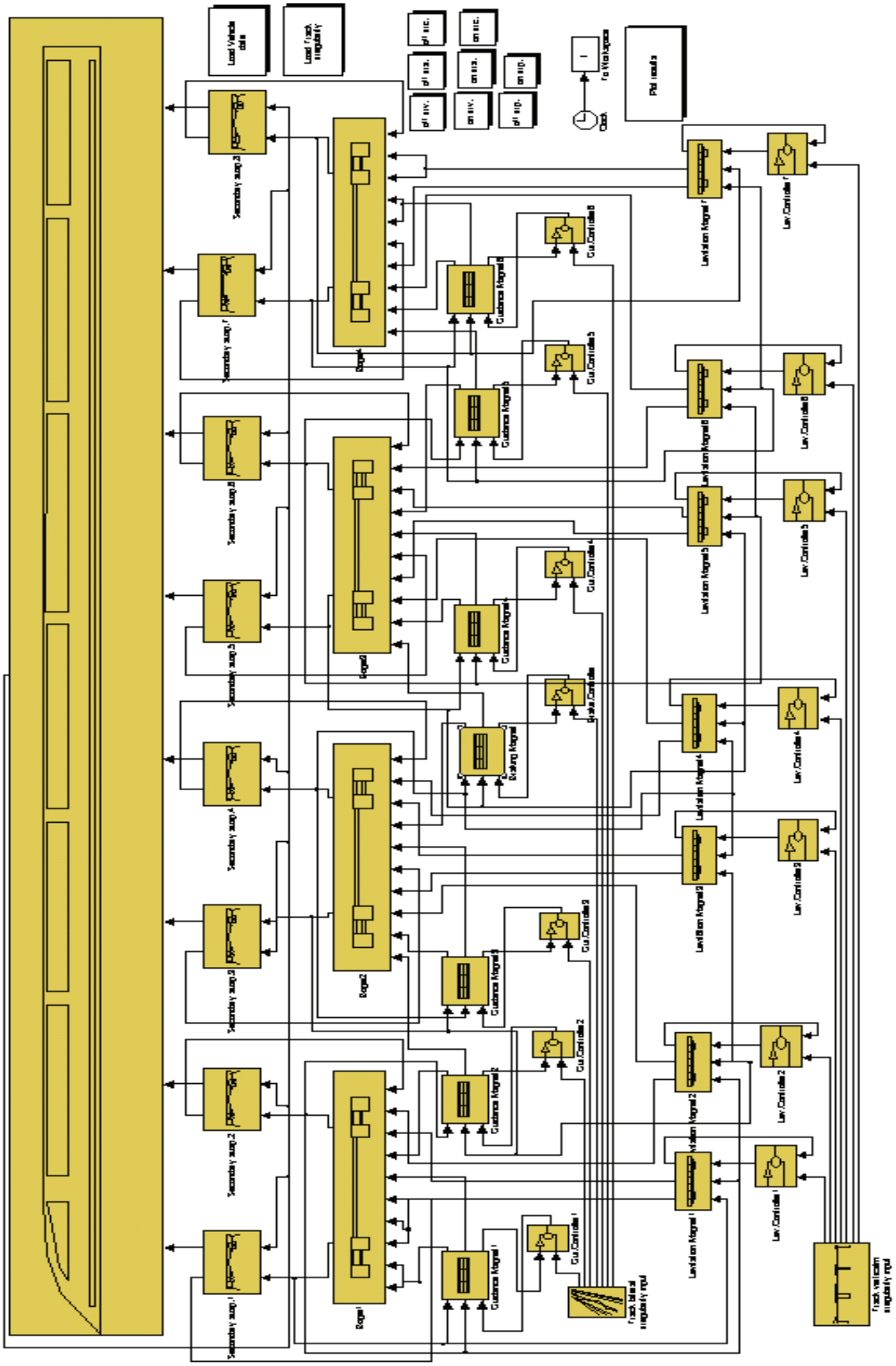

Fig.5: SIMULINK diagram of the vehicle simulation model

band [6], generally trend of the PSD curves of the irregularities are similar. At the moment there is no sufficient data collected, so a piece of measured railway track irregularities with a reduction of 1 over 4 in magnitude has been used in this paper. The peak periodical deformation of the guiding track is assumed to be 2 mm in the form of sine wave. The deformation of guiding tracks with 24 m in each length is shown at the top of Figure 7 for the first 1000 m. The following curves are vertical and lateral random irregularities of the centre line of the track, and the last is the track cross-level irregularity.

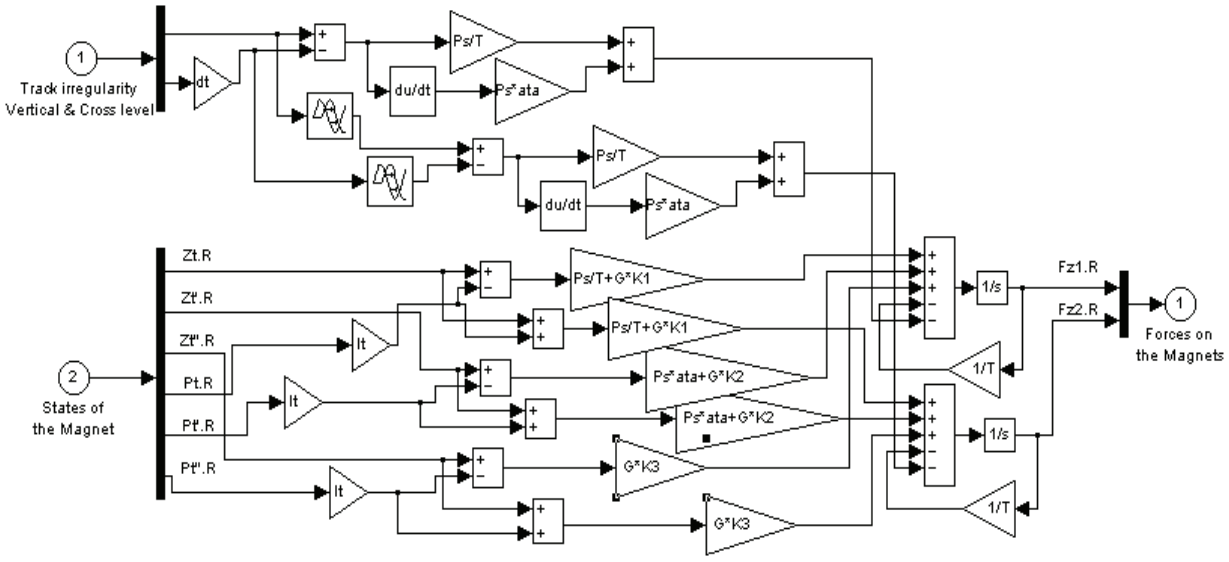

Fig.6: SIMULINK diagram of the block with the controller

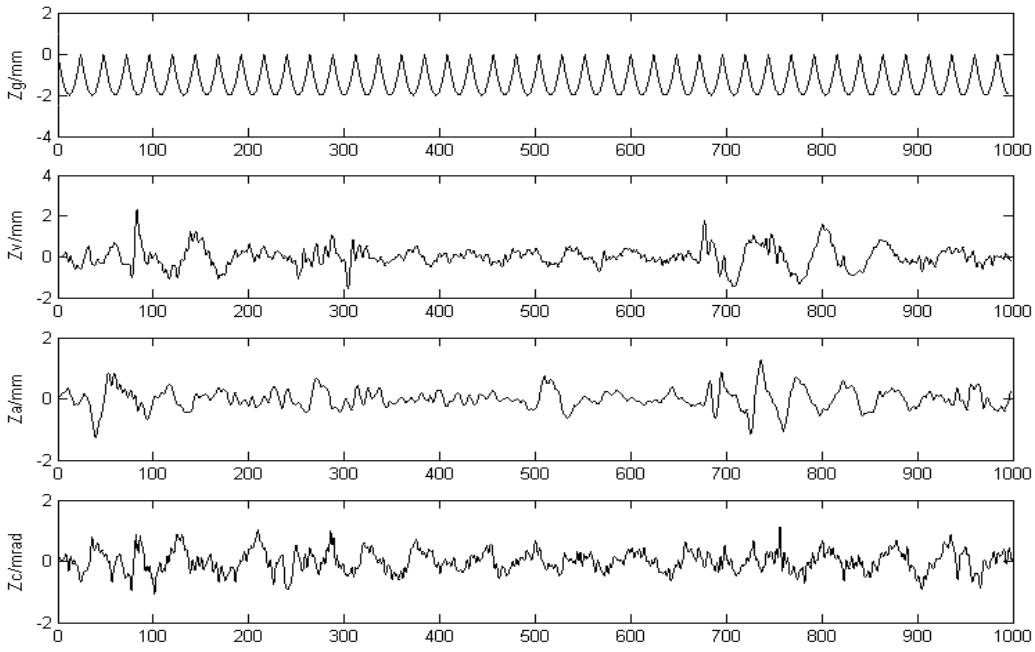

Fig.7: Space history of track irregularities

4.2 Main Simulation Results

Optimization of the suspension parameters has been made by the calculation of responses of the vehicle to the above track input. With the optimized suspension parameters, a typical accelerations of car body are illustrated in Figure 8, and the gap disturbances between magnet and track are illustrated in Figure 9. The time domain results for individual control and modal control are approximately similar.

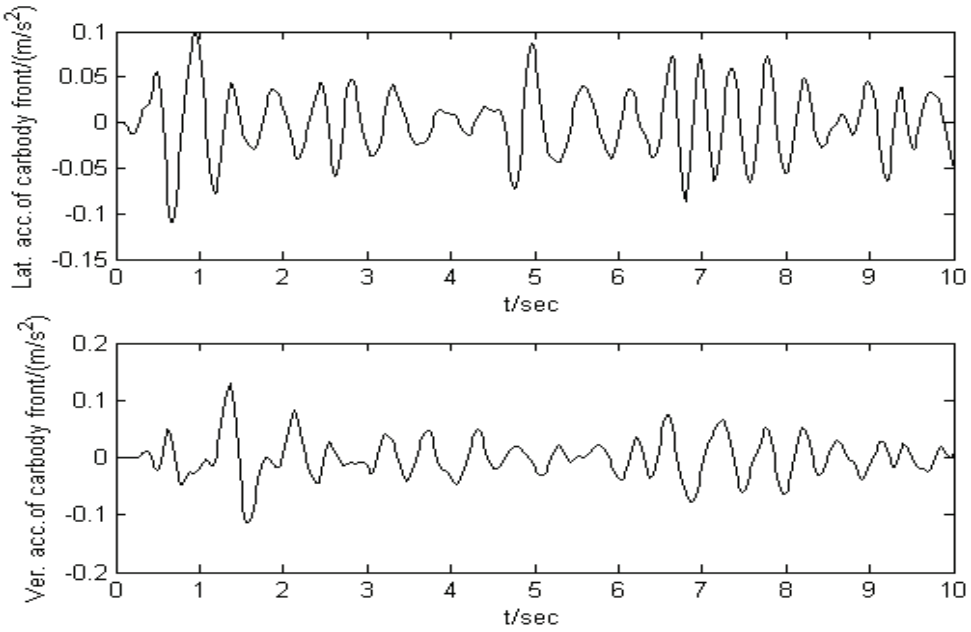

Fig.8: Lateral and vertical accelerations of a car body

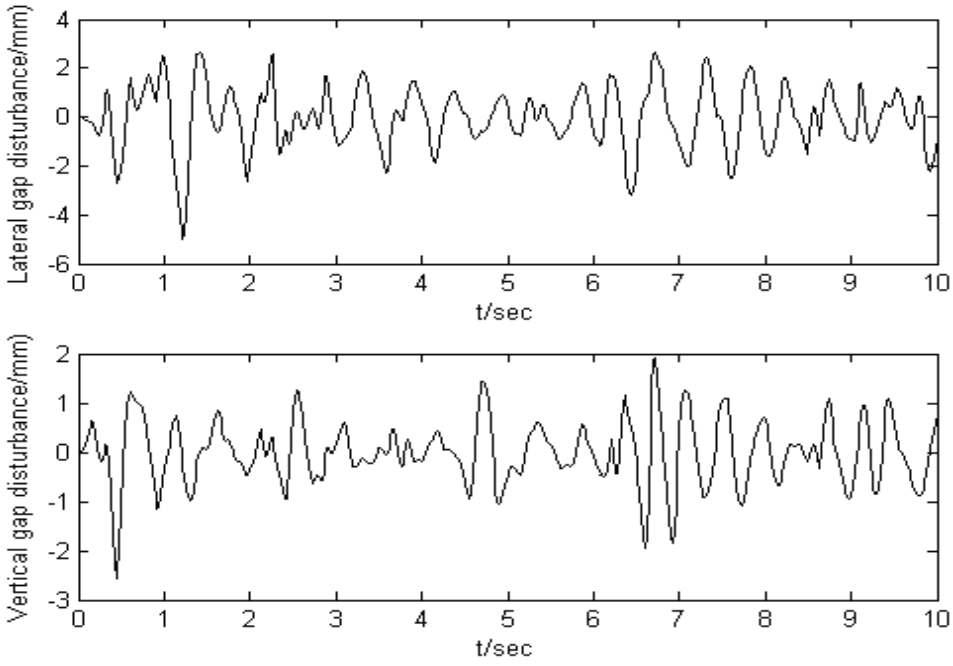

Fig.9: Lateral and vertical gap disturbances of magnet

5. Conclusions

For the purposes of investigation of different control strategies and ride performance of vehicle for both vertical and lateral directions a practical MAGLEV vehicle model is created. The control system design was carried out with a simple single mass model using Linear Quadratic Control. Employing MATLAB/SIMULINK, a computer simulation model with 93 DOF of mechanical system and 52 states for eletro magnet forces has been created to ensure high calculation efficiency. Reasonable results are obtained for optimization of suspension parameter and dynamic performances of the MAGLEV vehicle with optimal controllers for minimized energy consumption.

References

[1] E. Gottzein, B.O. Lange: Magnetic Suspension Control Systems for the MBB High Speed Train, Automatica, Vol. 11 (1975), pp.271-284.
[2] D.A. Limbert, H.H. Richardson, D.N. Wormely: Controlled Dynamic Characteristics of Ferromagnetic Vehicle Suspensions Providing Simultaneous Lift and Guidance, Journal . Syst. Meas. Control, Trans, ASME, 1979, 101(9), pp.217~222.
[3] X.J. Zheng, J.J. Wu, Y.H. Zhou: Numerical Analysis on Dynamic Control of Five-Degree-of-Freedom Maglev Vehicle Moving on Flexible Guideway, Journal of Sound and Vibration, 235(1), August 2000, pp.43-61.
[4] H. Coffey, J. Solinsky, J. Colton, J. Woodbury: Dynamic performance of the SRI Maglev vehicle, IEEE Transaction on Magnetics, Vol.10, 3, 1974, pp.451-457.
[5] R. Meisinger: Control Systems for Flexible Maglev Vehicle Riding over Flexible Guideway, IUTAM Symposium on the Dynamics of Vehicles on Roads and Railway Tracks, Amsterdam, Netherlands, 1975, pp.531~554.
[6] C F. Zhao, W.M. Zhai: Maglev Vehicle/Guideway Vertical Random Response and Ride Quality, Vehicle System Dynamics, 38(3), 2002, pp.185-210.
[7] Y.D. Xie, W.S. Chang: Modelling and Simulation of Electromagnetic Suspension Vehicle System(EMS) in Vertical Direction, Journal of the China Railway Society, 18(4), 1996, pp.47-54.
[8] C.F. Zhao, W.M. Zhai, Q.C. Wang: Simulation Analysis of the Dynamic Response of Low-speed Maglev Vehicle Curve Negotiation, China Railway Science, 26(3), 2005, pp.94-98.
[9] H. Ohsaki, R. W. Early, E. Suzuki: Numerical Simulation of the Vehicle Dynamics of the Superconducting Maglev System, The 16th International Conference on Magnetically Levitated Systems and Linear Drives, Rio de Janeiro, pp.230-235.
[10] Y.Q. Deng, S.H. Luo: Stability Research and Simulation of a Single Magnetic System, Electric Locomotives & Mass Transit Vehicle, 28(5), 2005.
[11] H.J. Hong, J. Li, S.J. Li: Kinematics Simulation of Maglev Train Based on Virtual Prototype, Electric Drive for Locomotives, 2005, pp.40-44.
[12] R. Meisinger: Beitraege zur Regelung einer Magnetschwebahn auf elastischem Fahrweg. Dr.-Ing. Dissertation, TU Muenchen 1977.
[13] R. Meisinger: Ermittlung der Bewegungsgleichungen eines electromechanischen Systems mittels LAGRANGE-Funktion. Schriftenreihe Helf 3, Georg-Simon-Ohm Fachhochschule Nuernberg (1999) S. 2-5.
[14] SHU Guangwei, CHEN Weigong, R. Meisinger: The Research on the Model of a Magnetic Levitation System [J].Electric Machine and Control, 2005: pp.187-190.
[15] R. Meisinger, Shu Guangwei, Cui Ziwei: Simulation of MAGLEV System with MATLAB/Simulink. Proceedings of Asian Simulation Conference / the 5th International Conference on System Simulation and Scientific Computer, Beijing : International Academic Publishers /Beijing World Publishing Corporation, 2002,pp.499-502.